Asik, D., Yagci, M.B., Duman, F. D. and Acar, H. Y. (2016) One step emission tunable synthesis of PEG coated Ag 2 S NIR quantum dots and the development of receptor targeted drug delivery vehicles thereof. Journal of Materials Chemistry B, 4(11), pp. 1941-1950.

There may be differences between this version and the published version. You are advised to consult the publisher's version if you wish to cite from it.

http://eprints.gla.ac.uk/178559/

Deposited on: 24 January 2019

Enlighten – Research publications by members of the University of Glasgow
http://eprints.gla.ac.uk

Journal of Materials Chemistry B

Accepted Manuscript

This is an *Accepted Manuscript*, which has been through the Royal Society of Chemistry peer review process and has been accepted for publication.

Accepted Manuscripts are published online shortly after acceptance, before technical editing, formatting and proof reading. Using this free service, authors can make their results available to the community, in citable form, before we publish the edited article. We will replace this *Accepted Manuscript* with the edited and formatted *Advance Article* as soon as it is available.

You can find more information about *Accepted Manuscripts* in the Information for Authors.

Please note that technical editing may introduce minor changes to the text and/or graphics, which may alter content. The journal's standard Terms & Conditions and the Ethical guidelines still apply. In no event shall the Royal Society of Chemistry be held responsible for any errors or omissions in this *Accepted Manuscript* or any consequences arising from the use of any information it contains.

ROYAL SOCIETY OF CHEMISTRY

www.rsc.org/materialsB

Table of Contents Graphic and Synopsis

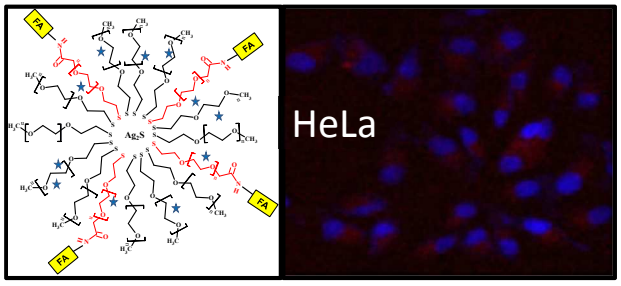

Emission tunable Ag_2S-PEG-Folic acid QDOTs synthesized in a single step in water are effective theranostic nanoparticles.

Journal of Materials Chemistry B Accepted Manuscript

Journal Name

ARTICLE

One step emission tunable synthesis of PEG coated Ag_2S NIR quantum dots and the development of receptor targeted drug delivery vehicles thereof

Received 00th January 20xx,
Accepted 00th January 20xx

DOI: 10.1039/x0xx00000x

www.rsc.org/

D. Asik,[a] M. B. Yagci,[b] F. Demir Duman[a] and H. Yagci Acar [a,b,c]

PEGylation of quantum dots (QD) to decrease their toxicity, increase blood circulation time, reduce non-specific uptake and also to solubilize and stabilize hydrophobic QDs in aqueous medium is a widely used approach and many different methods were developed to achieve this. QDs that are luminescent in the near-infrared region (NIR) has emerged recently as the more appropriate materials for bio-imaging studies. In this work, we describe s single step emission tunable aqueous synthesis of PEGylated Ag_2S NIRQDs. They are highly cytocompatible, not only due to PEG coating but also due to intrinsic biocompatibility of Ag_2S, in a single step aqueous preparation method using thiolated PEGs as the only coating material. Tuning emission wavelength within the medical window (775-930 nm) with quantum yield between 2-65 % is achieved by changing the reaction variables such as PEG molecular weight, pH and precursor ratios. Ag_2S-PEG NIRQDs prepared from 5kDa MPEG-SH at acidic pH provided a dramatic enhancement in the luminescence intensity. These NIRQDs were also designed with surface functional groups to attach folic acid and loaded with Doxorubicin (DOX) which dramatically enhanced uptake and efficacy of DOX (50% cell death with 15 nM DOX) in FA-receptor overexpressed cancer cell lines (HeLa). They also showed strong cytoplasmic NIR signal in the in vitro studies, demonstrating a great theranostic potential.

Introduction

Cancer is one of the most serious diseases at the present time. Even though there are many private and public research institutions heavily working on early diagnosis of cancer and development of vaccine and therapeutic agents, cancer is still one of the most deadly diseases in the world. Multifactorial and multifarious nature of cancer makes the fight against cancer difficult. Early diagnosis, effective and selective delivery of chemotherapeutic drugs to the tumor site are all imperative for successful cancer therapy.

Nanoparticles are usually capable of doing couple of tasks at the same time, such as drug delivery in addition to imaging, therefore has great potential in diagnosis and therapy.[1-5] Quantum dots are being investigated for imaging and labelling as well as for drug and gene delivery.[3, 6-9] Unique properties including size tunable emission, absorption in a broad but emission in a narrow window coupled with long luminescence lifetime make semiconductor quantum dots (QDs) as preferred materials for optical imaging and labeling.[3, 10-13] QDs are synthesized from group II-VI, III-V and IV-VI atoms. Group II-VI quantum dots such as CdS, CdSe, CdTe, ZnSe are excited in UV and luminesce in the visible range (400-700 nm).[14] These are the most studied quantum dots. Even though these quantum dots luminesce strongly with a very sharp emission peak, there are significant drawbacks in their practical use in medicine. Most significant problems are the potential damage due to UV-irradiation, the autofluorescence of the living tissue in the visible region, absorption of visible light by biological components such as hemoglobin and water, and the limited penetration depth of the visible light.[15, 16] In recent years, emission in the near infrared (NIR), especially, 700-900 nm is suggest as the more appropriate window for biological applications.[15, 17] Another important issue is the cytotoxicity of QDs, especially for the in vivo use. For example, there are CdHgTe/CdS,[18] CdSeTe/CdS,[19] and PbS[20] NIR quantum dots with emission in the desired medical window but they are composed of heavy metals such as Cd and Pb which are considered as toxic.[21-25] The most widely used method to decrease toxicity of Cd-based quantum dots, is the over coating with biocompatible polymers, usually polyethylene glycol (PEG).[11, 12] PEG is often attached to the end groups of the primary coating of the QD through ester or amide linkages.[26-28] Alternatives such as InAs/InP/ZnSe[29], $CuInS_2$/ZnS[30, 31] are being developed but there is no wide selection of heavy-metal free NIR emitting QDs.

[a] Koc University, Graduate School of Materials Science and Engineering, Rumelifeneri Yolu, 34450-Sariyer, Istanbul-Turkey.
[b] Koc University, Surface Science and Technology Center (KUYTAM), 34450-Sariyer, Istanbul-Turkey.
[c] Koc University, Department of Chemistry, Rumelifeneri Yolu, 34450-Sariyer, Istanbul-Turkey.

† Electronic Supplementary Information (ESI) available: Materials, size and surface charge data, absorbance spectra, time dependent PL spectra, curve fitting, EDX, DOX calibration curve, determination of DOX concentration, toxicity data at high dose and cell morphology. See DOI: 10.1039/x0xx00000x

Journal of Materials Chemistry B Accepted Manuscript

Please do not adjust margins

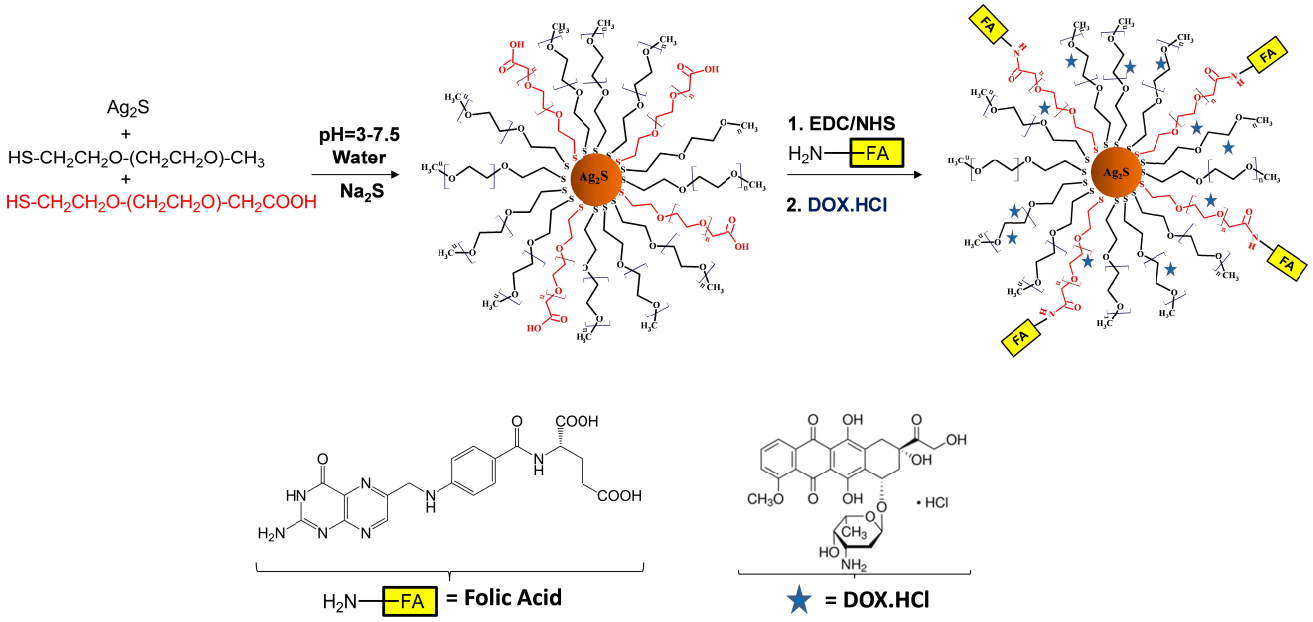

Scheme 1. Schematic representation of aqueous synthesis of functional Ag_2S-PEG QDs, folic acid conjugation and DOX loading.

Ag_2S quantum dots emit in the infrared region and are highly cyto- and hemocompatible even without PEGylation.[13, 32-34] Yet, PEGylation has some other benefits such as enhanced colloidal stability due to steric stabilization, increased blood circulation time and decreased non-specific uptake of nanoparticles.[27, 35] PEGylated materials are also used for the transfer of hydrophobic QDs into water.[12] Hydrophobic Ag_2S luminescent in the NIR-II has been also rendered hydrophilic through either an interdigitated bilayer formed with a PEGylated amphiphilic polymer[36] or by ligand exchange with dihydrolipoic acid which is later conjugated to PEG by Wang *et al*.[37] This usually caused a red shift in the emission maxima and broadening of the peak. More importantly, Ag_2S QDs used in these studies are prepared by decomposition of silver dithiocarbamates at high temperatures (above 200°C).[38] This method lacks emission tunability and the highest quantum yields reported is 15 % (with respect to IR-26 with 0.5% QY).[33] Synthesis of QDs directly coated with PEG has been reported by Eychmuller *et al.* for CdTe using short PEG chains (MPEG750SH) both in organic and aqueous medium[39] but size tunability was achieved only in polar protic solvents under reflux.[40]

Therefore, here we aim emission tunable synthesis of biocompatible quantum dots with PEG coating that are strongly luminescent in the NIR-I window in a simple, single step aqueous synthesis. This is achieved by in situ coating of Ag_2S with MPEG-SH in an aqueous synthesis method. In order to optimize the quality of Ag_2S QDs and tune the emission wavelength, reaction variables such as Ag/S and coating/Ag mole ratios, reaction pH, and molecular weight of MPEG-SH (2 and 5kDa) were studied. Since, in general, PEG increases the blood circulation time and decreases the non-specific uptake by cells; it is preferable to tag PEGylated particles that will provide receptor specific internalization of the particles. Therefore, PEG-Ag_2S particles with –COOH surface functionalities were prepared in the same way and decorated with folic acid to direct QDs to cancerous cells via overexpressed folate receptors (Scheme 1). Cytocompatibility of these QDs were tested on HeLa cells, demonstrating highly cytocompatible nature of the QDs. In addition, chemotherapeutic Doxorubicin has been loaded electrostatically to these QDs, to demonstrate the ability of Ag_2S-PEG NIRQDs as drug delivery vehicles. NIR luminescence provided an effective optical detection of QDs in the cytoplasm of cells, indicating formation of a promising new theranostic nanoparticles.

Experimental

Materials

All reagents were purchased at the highest purity or reagent grade and used without further purification. Silver nitrate ($AgNO_3$), folic acid, DMEM medium (with 10% fetal bovine serum, 1% penicillin-streptomycin antibiotic solution, 4 mM L-glutamine and phenol red) were purchased from Sigma-Aldrich. Sodium sulfide (Na_2S) was purchased from Alfa-Aesar. Functional PEGs (MPEG-SH 5000, MPEG-SH 2000 and CMPEG-SH 2000) were purchased from Laysan Bio, Inc. Doxorubicin hydrochloride was purchased from BioChemica. Sodium hydroxide and ethanol were purchased from Merck. Acetic acid was purchased from Lachema. Dimethyl sulfoxide (DMSO) was purchased from VWR. Ethanol (EtOH) was purchased from Merck. 1-(3-Dimethylaminopropyl) carbodiimide hydrochloride, 98% was purchased from Alfa Aesar and N-hydroxysuccinimide was purchased from Aldrich. Trypsin–EDTA was purchased from MULTICELL and 4%

Journal of Materials Chemistry B Accepted Manuscript

This journal is © The Royal Society of Chemistry 20xx

Please do not adjust margins

paraformaldehyde was purchased from Chemcruz. 4,6-Diamidino-2-phenylindole dihydrochloride (DAPI) was purchased from Sigma Aldrich. Phosphate buffered saline (PBS) tablet was purchased from Sigma and fetal bovine serum (FBS) was purchased from Capricorn. LDS 798 near-IR laser dye (Quantum yield reported as 14% in DMSO by the producer) was purchased from Exciton Inc. Milli-Q water (18 mOhm) was used as a solvent. MTT (3-(4,5-dimethylthiazol-2-yl)-2,5-diphenyltetrazolium bromide) was purchased from AppliChem.

Synthesis of PEG Coated Ag_2S Quantum Dots

A typical preparation method for Ag_2S-PEG NIRQDs is as follows: Silver nitrate (0.0625 mmol $AgNO_3$) was dissolved in 20 mL deoxygenated deionized water in a three-neck round-bottom flask fitted with Argon inlet/outlet. Thiolated polyethylene glycol (e.g. 0.1 mmol; MPEG-SH MW 2000) was added to this solution under vigorous mechanical stirring. pH of the solution was adjusted to desired value (3 or 7.5) with acetic acid (CH_3COOH) and heated up to 90°C. Na_2S (0.0156 mmol) was dissolved in 5 mL deoxygenated water in a separate round bottom flask and transferred slowly into the reaction solution via a cannula using Argon purge under vigorous mechanical stirring. After desired amount of time necessary for the growth of QDs, solutions were cooled to room temperature. After being washed with MilliQ water using Amicon-Ultra centrifugal filters (3,000 Da and 10,000 Da cut off for mPEG 2kDa and 5kDa, respectively), QD solutions were stored at 4 °C in dark. Particle growth was followed by absorbance and photoluminescence measurements of the aliquot taken from the reaction mixtures at different time points.

For the synthesis of –COOH functional nanoparticles, a mixture of 70/30 mol ratio of MPEG-SH/CMPEG-SH was used in the formulation.

Synthesis of Folic Acid Conjugated QDs (QD-FA)

0.18×10^{-4} mmol EDC and 0.18×10^{-3} mmol NHS were dissolved in distilled water (pH 8.8) and then added into 15 mL quantum dot (QD9 in Table 1) solution which has 30 % CMPEG-SH (0.18×10^{-4} mmol CMPEG-SH) in the coating formulation and the mixture was stirred for 5 min at room temperature for the activation of carboxylic acids. Then 0.18×10^{-4} mmol folic acid (FA) was added in to this solution and stirred overnight at RT. FA conjugated QDs were subjected to dialysis (3K molecular weight cut-off cellulose dialysis membrane, CelluSep T1 Regenerated Cellulose Tubular Membrane, Spectrum labs.) in distilled water over 2 days for the removal of excess chemicals and by-products.

Preparation of Doxorubicin Loaded QDs

For the preparation of QD-FA-DOX, 0.1 mL doxorubicin hydrochloride (DOX) solution (pH 5.5; 0.22 mg/mL) was mixed with 3 mL QD-FA quantum dots (QD9-FA at 196.5 µg/mL Ag concentration) at pH 6. For the preparation of QD-DOX, 0.5 mL DOX solution (pH 5.5; 0.22 mg/mL) was electrostatically loaded into 1.5 mL PEG coated Ag_2S quantum dot (QD9 at 331 µg/mL Ag concentration). DOX loaded QDs were washed through 3K Amicon centrifugal filter tubes with fresh DI water to remove unbound DOX.

Cell Culture

Human cervical carcinoma (HeLa) and mouse fibroblast cells (NIH-3T3) were cultured in complete DMEM medium consisting of 10 % fetal bovine serum, 1 % penicillin-streptomycin antibiotic solution and 4 mM L-glutamine. Both cell lines were incubated at 37 °C under 5 % CO_2. Cell passage with fresh medium is performed once in two days. Trypsin-EDTA was used for cell detachment process. Paraformaldehyde was used to fix the cells on the 6 well plates for microscopic images. DAPI was used for labelling the cell nuclei.

Cell Viability

Human cervical carcinoma (HeLa) and mouse fibroblast cells (NIH-3T3) were cultured at a $1x10^4$ cells/well in 96-well plates in complete DMEM, as described above. The medium (200 µL) was replaced with fresh medium (after 24 hours) and charged with nanoparticles at doses between 5-50 µg Ag/mL and incubated for 24 hours. For cell viability assessment, 5 mg/mL MTT solution in 1 M PBS was prepared. After 24 hour incubation with nanoparticles, the medium (containing the un-internalized nanoparticles and dead cells, if any) in each well was replaced with 150 µL complete DMEM medium and 50 µL of MTT solution. After 4 hour incubation the medium was removed and 200 µL DMSO:EtOH (1:1) solution was added to each well to dissolve purple colour formazan product that indicates the number of viable cells. Formazan amount was quantified by its absorbance intensity at 600 nm and 630 nm (ELx800 Biotek Elisa reader). The absorbance value at 630 nm

Table 1. Formulation and Properties of Ag_2S-PEG QDs

Rxn Code	SH/Ag/S[a] (mole ratio)	Mwt[b] (g/mol)	pH	Time (min)	Emission λ_{max} (nm)	QY[c] (%)	D[d] (nm)	Band Gap (eV)
QD1	6.4 / 4 / 1	2000	7.5	90	847	8.6	2.3	1.81
QD2	6.4 / 2 / 1	2000	7.5	120	915	6.1	2.6	1.55
QD3	6.4 / 6/ 1	2000	7.5	90	775	1.9	2.2	1.86
QD4	10 / 5 / 1	2000	7.5	90	860	10.7	2.5	1.59
QD5	5.12 / 4 / 1	2000	10	90	798	2.4	2.3	1.82
QD6	6.4 / 4 / 1	5000	3	90	930	65.6	2.5	1.58
QD7	6.4 / 4 / 1	5000	7.5	90	890	12.0	2.6	1.55
QD8	6.4 / 4 / 1	2000	3	90	930	29.4	2.6	1.56
QD9*	6.4 / 4 / 1	2000	2.8	90	925	17.3	2.6	1.55

[a]0.64 mM Na_2S concentration, [b]Molecular weight of PEG in MPEGSH, [c]Quantum yield calculated with respect to LDS 798 near-IR dye, [d]Particle sizes calculated by Brus equation using the absorbance onset (Figure S1 in SI).[1, 2] *30 mol % of the organic coating is HS-PEG-COOH.

Journal of Materials Chemistry B Accepted Manuscript

was subtracted from the absorbance value at 600 nm. Percent viability was determined by comparing absorbance average of five replicates for each dose and absorbance average of control cells with no nanoparticle exposures. Statistical analysis was performed by one-way ANOVA with Tukey's multiple comparison test of the Graph Pad Prism 5 software from GraphPad Software, Inc., USA.

Cell Imaging

Human cervical carcinoma (HeLa) cell lines were cultured at $2x10^4$ cells/well in 6-well plates in complete DMEM culture medium overnight, then the medium was replaced with fresh DMEM and nanoparticles at 10 µg Ag/mL dose. After 6 and 24 hours of incubation, the medium was discarded and the cells were washed with PBS (1 M) three times. Then, 1 mL paraformaldehyde was added to each well and stored in dark to fix cells. Following this procedure, paraformaldehyde was discarded and each well was washed with 1 M PBS for three times. 1 mL PBS was left in each well. The fixed cell samples were examined under Inverted Life Science Microscope at 20× magnification (Olympus-Xcellence RT Life Science Microscopy). Three different filters that were specific for Cy3 (λ_{exc}: 513 - 556 nm and λ_{em}: 570-615 nm), DAPI (λ_{exc}: 352-402 nm and λ_{em}: 417-477 nm) and NIR region (λ_{exc}: 550 nm and λ_{em}: 650 nm long pass) were used to image the cell nuclei, QDs and DOX. Same experimental procedure was also performed for control cells with no nanoparticles.

Characterization

Dried samples were used for the XRD and XPS analysis. D8 Advance Bruker instrument with Cu K-alpha radiation (λ=1.5406 Å) was used for XRD. Powdered samples placed on the glass with a double sided sticky type and 2θ angles between 10^o-80^o was recorded. Powdered samples were placed on an aluminium type for the XPS analysis performed with Thermo Scientific K-Alpha XPS with Al K-alpha monochromatic radiation (1486.3 eV). Pass energy of 50.0 eV and 400 mm spot size was used for the analysis. Take-off angle (surface normal with respect to analysis detector) was 90°. All spectra were corrected according to C1s=284.5 eV.

FTIR spectrum was recorded on a Thermo Scientific Nicolet iS10 instrument (ATR-FTIR) in the wavenumber range of 400-4000 cm^{-1} for functional group analysis.

Shimadzu 3101 PC UV-Vis-NIR spectrophotometer was used for the absorbance measurements in the 300–700 nm range. Crystal size of Ag_2S crystals were calculated from the absorbance onset using Brus equation (Eqn. 1).[41, 42]

$$\Delta E = \frac{\hbar^2\pi^2}{8R^2}\left[\frac{1}{m_e}+\frac{1}{m_h}\right]-1.8\frac{e^2}{\varepsilon_{Ag_2S}4\pi\varepsilon_0 R} \qquad \text{Eqn. 1}$$

Where $\Delta E=E_{bulk}-E_{sample}$, m_e (0.286 m_0) and m_h (1.096) are the effective electron and hole masses for Ag_2S, respectively, ε (5.95) is the dielectric constant of Ag_2S and R is the radius of the nanocrystal.

Photoluminescence spectra was recorded on a home-made instrument with gold reflector, 0.5 m Czerny-Turner monochromator and silicon detector that is sensitive over the wavelength range of 400-1100 nm. A continuous-wave, frequency doubled Nd:vanadate laser operating at 532 nm was used as the excitation source. The luminescence signal was filtered using a 590 nm long pass filter. Si detector with femtowatt sensitivity (Thorlabs PDF10A, 1.4×10^{-15} W $Hz^{-1/2}$) was used. For these measurements slid width was set to 0.2 nm. Quantum yield (QY) of nanoparticles were calculated based on the procedures detailed in the literature.[43, 44] Briefly, samples of aqueous QD solutions and LDS 798 NIR dye in methanol (QY reported as 14 % by the producer) were prepared at three different concentrations providing similar absorbance values at the excitation wavelength of 532 nm, keeping the absorbance at and below 0.1. Integrated areas under the emission curve for each were plotted against the absorbance and QY (ϕ) of the QDs was calculated from the gradients of these plots, using the refractive index of the water and MeOH based on equation 2.

Eqn. 2

$$\emptyset_{QD} = \emptyset_{St}\,(Grad_{QD}/Grad_{St})\,(n^2_{QD}/n^2_{St})$$

TEM analysis was done at UNAM, Ankara. A dilute solution of QDs were dropped on a carbon coated Cu-grid and evaporated. FEI Tecnai G2 F30 TEM operated at 200 kV was used for the high resolution images. EDX was done at 15° tilt angle.

Hydrodynamic size and zeta potential measurements of the aqueous colloidal Ag_2S-PEG QDs were performed by Malvern zetasizer nano ZS.

Ag^+ content of the quantum dot solutions were determined by Spectro Genesis FEE Inductively Coupled Plasma Optical Emission Spectrometer (ICP OES) based on reference curve that was created by standard solutions. For the ICP analysis, QD solutions were treated with a nitric acid/sulfuric acid mixture and diluted with DI water.

Results and Discussion

Synthesis and Characterization of Ag_2S NIRQDS

Development of emission tunable synthesis of functional PEGylated, heavy-metal free quantum dots (Ag_2S) with near infrared emission is aimed for theranostic use of quantum dots. In a simple, one-step, economic, and safe synthetic method, Ag_2S quantum dots were prepared from Ag^+ and S^{2-} salts in water in the presence of MPEG-SH (Scheme 1). Particle size and hence the emission was tuned with combination of reaction time, stoichiometry, pH and the molecular weight of the polymer (Table 1). Colloidally stable QDs with emissions centred between 775-930 nm with about 65-70 nm difference in the peak maxima are obtained. For a given formulation, peak maximum of the emission did not change significantly with the reaction time but the intensity did (Figure S2 in

Journal of Materials Chemistry B Accepted Manuscript

This journal is © The Royal Society of Chemistry 20xx

Please do not adjust margins

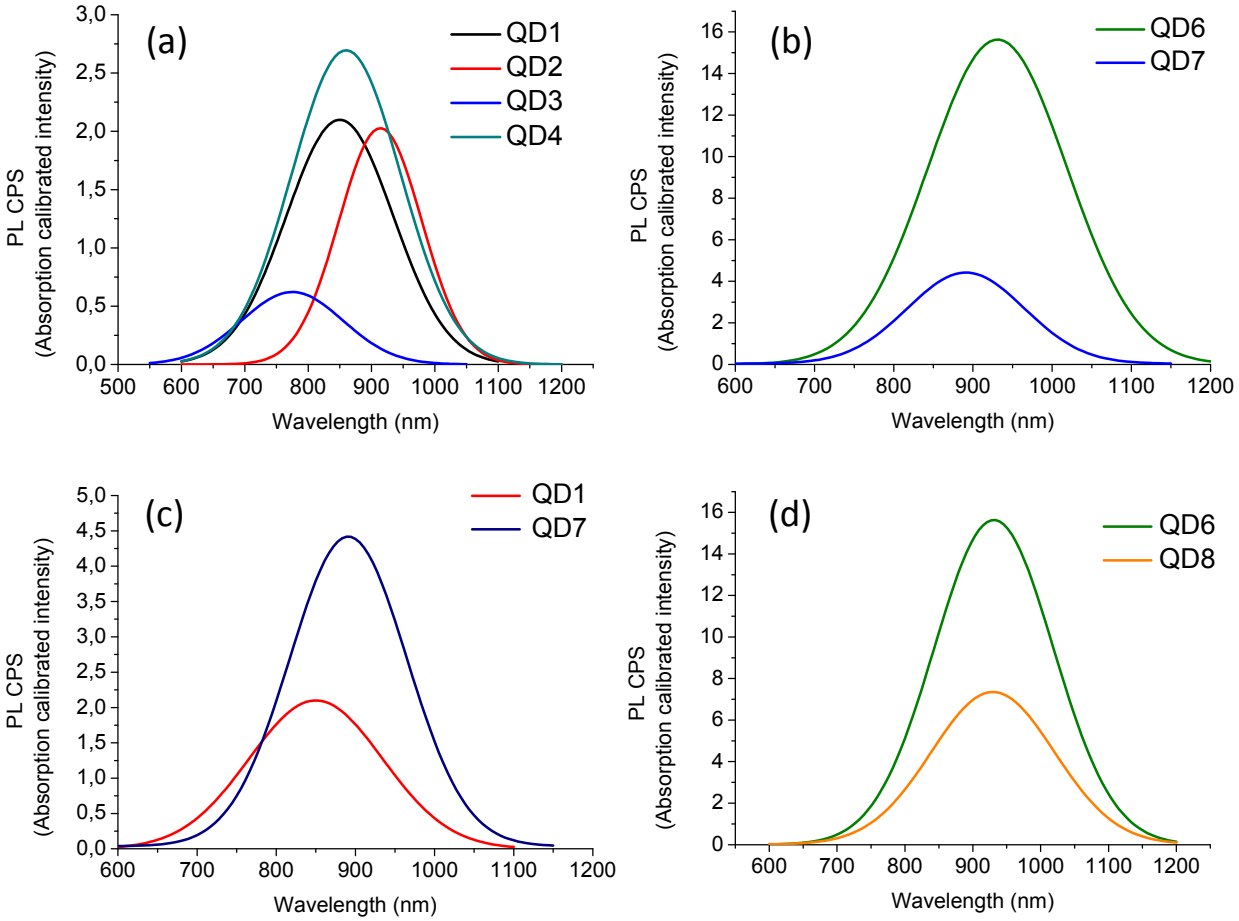

Fig. 1 Absorbance calibrated photoluminescence spectra of Ag_2S-PEG QDs. *Due to limitation in the detection range (600-1050 nm) of the detector, emission spectra are plotted by curve fitting formula of OriginPro 9.0 software (Detailed in Figure S3 in the SI).

Supporting Information, SI). This is rather typical for Ag_2S synthesized with Na_2S.[32, 33]

As seen in Figure 1a, keeping everything else the same, as Ag/S ratio increases (QD1, QD2 and QD3), particles are captured at a smaller size. Yet, smallest particle (QD3: Ag/S=6/1) with emission maximum at 775 nm showed significantly lower emission intensity. Smaller particles are affected more by the surface defects. In QD3 there is less MPEG-SH per Ag^+ (SH/Ag=1.06) compared to other two, which may cause a less effective surface coating and hence surface defects. QD1 and QD2 had SH/Ag ratio of 1.6 and 3.2 and about the same emission intensity. Based on this data, a fine tuning of the emission wavelength with strong emission intensity was achieved with a new formulation of Ag/S ratio of 5 and HS/Ag ratio of 2 (QD4), producing particles with emission maxima at 860 nm with 10 % QY, which is better than QD1 and QD2. Emission maxima around 850-860 nm are highly desirable for optical imaging studies, since routine confocal or fluorescent microscopes loose efficiency at longer wavelengths.

Reaction pH showed a dramatic impact on particle properties. Reducing the reaction pH to 3 from 7.5 caused a red shift of the emission maximum due to larger crystal size along with a dramatic increase in the quantum yield. For QDs prepared with PEG2000, luminescence maximum shifted from 847 to 930 nm and QY increased from 8.6 to 29.4 (QD1 and QD8) (Table 1). Same type of behaviour was observed when PEG5000 was used as a coating (QD6 and QD7): Emission showed 40 nm red shift with about 3.5 times increase in QY to 65.6 % (Figure 1b, Table 1). Larger crystal size may be due to better solubility of Ag_2S in acidic medium, making the critical stable particle size larger compared to reactions performed at neutral pH. Enhancement of luminescence intensity under acidic reaction conditions may be at least partially due to formation of different Ag-SR complex at acidic pH and more Ag-coordination with RSH since its deprotonation will be reduced as well.

Molecular weight of PEG showed a significant impact on particle properties, especially on the luminescence intensity. This may be due to the differences in polymer conformation on the particle surface. As seen in Table 1 and Figure 1c and 1d

Journal of Materials Chemistry B Accepted Manuscript

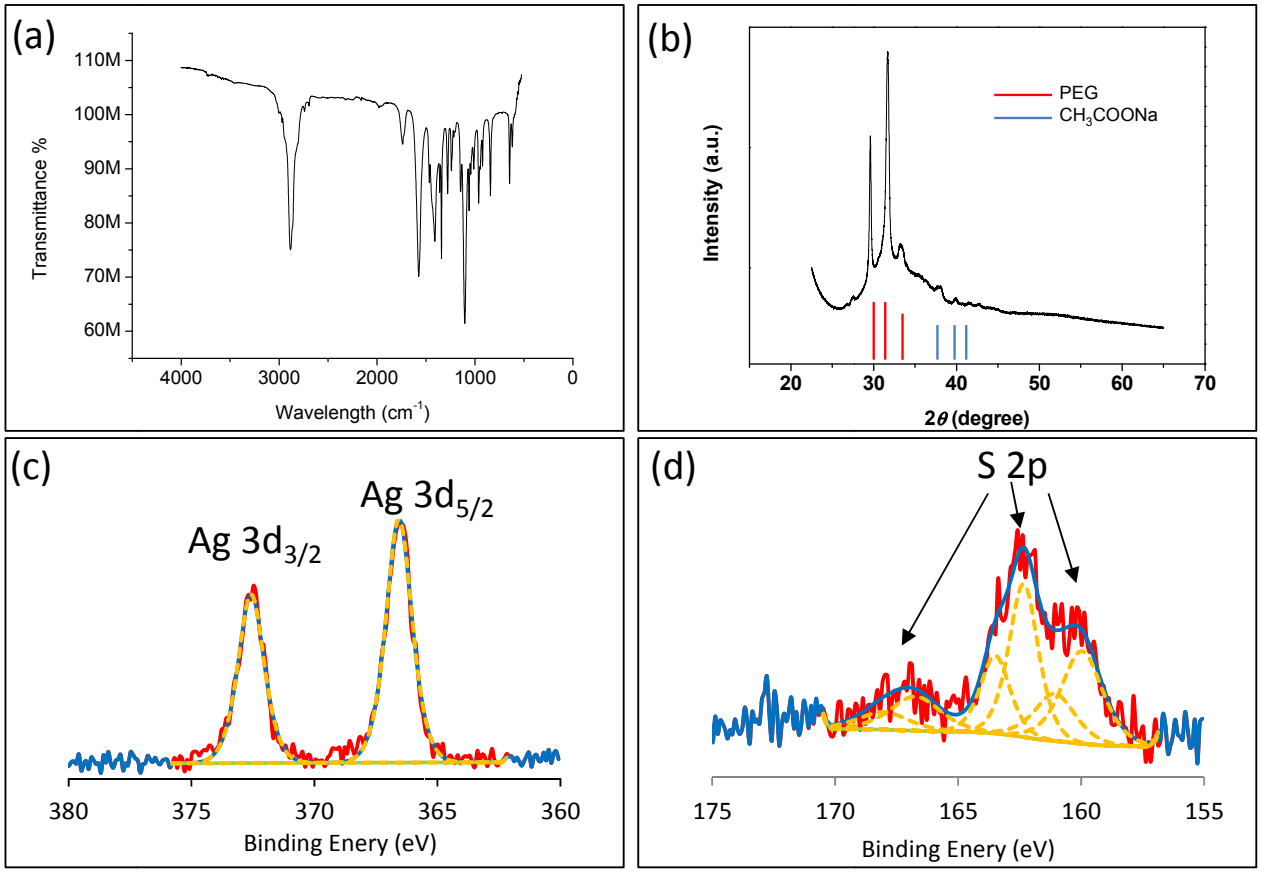

Fig. 2 (a) IR spectrum of Ag_2S-PEG (QD1) (b) XRD pattern of Ag_2S-PEG (QD6) and (c) Ag 3d and (d) S 2p XPS spectra of Ag_2S-PEG.

keeping all other parameters identical, increasing molecular weight of PEG from 2000 g/mol to 5000 g/mol, increased the QY about 40 % for particles synthesized at pH 7.5 with 43 nm red shift in peak maxima (QD1 and QD7). Increase in the size may be due to slower diffusion of the higher molecular weight polymer to the crystal surface and/or due to less dense surface coating, allowing easier diffusion of the ions to the crystal surface. When synthesis was performed at pH 3, increasing molecular weight of PEG showed a dramatic difference in the QY with more than 100 % increase (QD6 and QD8) reaching to 65 % QY. These QY values are quite high when compared to reported values in the literature for Ag_2S QDs. Gui *et al*. and Hu *et al.* reported about 15 % and 17 % QY[36, 45], respectively for the as-prepared Ag_2S QDs. Hocaoglu *et al.* reported as high as 39 % QY upon aging of Ag_2S QDs.[32]

IR spectrum of Ag_2S-PEG QDs indicates the absence of S-H stretching which is typically around 2550 cm^{-1}. Presence of C-O stretching at 1100 cm-1, C-H stretching at 2885 cm^{-1}, C-C stretching at 1575 cm^{-1} and 1414 cm^{-1} indicates the binding of MPEG-SH to crystal surface (Figure 2a).

Confirmation of Ag_2S crystal formation and determination of crystal type by XRD was difficult due to the small size of the crystals and the amorphous PEG coating. As seen in Figure 2b, major peaks observed in the diffractogram of QD6 is coming from the PEG. Although this sample was washed with fresh water couple of times, sodium acetate was detected, as well, possibly coming from the adsorbed acetate used in the synthesis. On the other hand, XPS analysis provides a strong support for the Ag_2S formation. Ag 3d5/2 signal at the binding energy of 366.57 eV and S 2p3/2 at 160 eV are typical for Ag_2S (Figure 2c-d). Presence of a second type of S 2p3/2 at 162.34 eV is due to the thiolated PEG coating and represents the organic C-S.

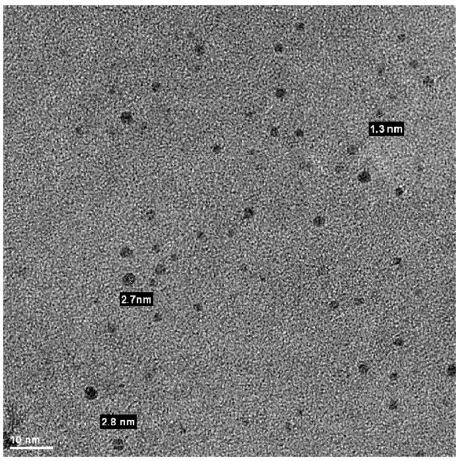

Fig. 3 TEM image of Ag_2S-PEG QD (QD8) at 10 nm scale.

Journal of Materials Chemistry B Accepted Manuscript

This journal is © The Royal Society of Chemistry 20xx

Please do not adjust margins

The small S 2p signal at 166.78 eV corresponds to an oxidized sulfur (SO_3^{2-}, SO_4^{2-}) which may be due to the aging of the sample.[46]

TEM images of these QDs showed non-aggregated nanoparticles with diameter between 1.7 to 2.5 nm (Figure 3). This is somewhat close to the calculated diameter of 2.6 nm by the Brus equation (Table 1). Discrepancy between the calculated and observed sizes has been reported previously.[13] Energy dispersive X-ray spectroscopy (EDS) confirms the presence of Ag, S and O (coming from PEG) (Figure S4 in the SI).

Hydrodynamic sizes of Ag_2S-PEG QDs in water are measured by Dynamic Light Scattering (DLS) and are mostly below 50 nm indicating ultrasmall sizes (Table S1 in the SI). If number average values are considered, they are at and below 12 nm. QD6 and QD7 coated with PEG5000 are the larger ones due to thicker polymeric shell. PEG5000 also caused broader size distribution, may be due to faster growth of the larger crystals. Zeta potential of these QDs is slightly negative, which is typical for PEGylated surfaces.[47]

Cytotoxicity Evaluation of Ag_2S-PEG NIRQDs

The cytotoxicity of two different Ag_2S-PEG NIRQDs to human cervical cancer cells (HeLa) and mouse fibroblast cells (NIH/3T3) were determined by the MTT assay which depends on the mitochondrial activity. QD3 which has an emission maximum at 775 nm (smallest particle) with PEG2000 coating and QD7 with emission maximum at 890 nm (longest wavelength that can be detected with the confocal microscope) with PEG5000 coating were used for the cytotoxicity evaluation as representative QDs. Cytotoxicity of $AgNO_3$ was also evaluated for comparison. Dose of the QDs were calculated based on their Ag content measured by ICP-OES. Between 5-25 µg/mL Ag dose, no significant cytotoxicity was observed in either cell lines (corresponding to 1.7 mg QD/mL QD3 and 3.8 mg QD/mL QD7 concentration) (Figure 4A). However, at 25 µg/mL Ag dose, $AgNO_3$ is already very toxic. This indicates that silver ion does not leach out of the nanoparticle, at least in any significant dose. This is an expected result due to very low solubility of Ag_2S. Both QDs induced a significant drop in viability of NIH/3T3 cells but only at 50 µg/mL Ag (corresponding to 3.4 mg QD/mL QD3 and of 7.6 mg QD/mL QD7 concentration). Only the larger QD7 showed significant toxicity in HeLa cells at 50 µg/mL Ag. These indicate that QDs are more toxic to NIH/3T3 cells and smaller QDs are better tolerated by HeLa cells. Yet, in literature, the maximum Ag_2S (PEGylated) concentration used for the cytotoxicity assays is about 100 µg/mL.[33] Considering that Ag_2S-PEG QDs did not cause any drop in viability even in mg doses, these particles can be considered quite biocompatible. Especially, being non-toxic to healthy cell lines is an asset. It is highly desirable to use these QDs as a fluorescent probe and a drug carrier that is directed to cancer cells.

Receptor Targeted DOX Delivery with Ag_2S-PEG NIRQDs. Cancer drugs kill both healthy and cancerous cells. To reduce deadly effects of these drugs, targeted drugs are required. Due to overexpression of folate receptors on the surfaces of many types of human cancer cells compared to healthy cells, folic acid (FA) is chosen as the targeting ligand in this study.[48, 49] Folic acid (FA) has a strong binding affinity to folate receptors. In order to bind FA to the Ag_2S-PEG QDs, a new nanoparticle (QD9) with surface –COOH groups was prepared using CM-PEG-SH as 30 mol % of the coating material. FA was conjugated to the QD surface via amide bond using the standard EDC-NHS chemistry (Scheme 1). Quantification of FA conjugation is usually done based on the absorbance of FA at 295 nm but, due to strong absorbance of Ag_2S at this wavelength, luminescence peak of FA at 450 nm was used in this study (Figure S5 in the SI). The FA amount was calculated as 3.99×10^{-9} mol/mL of QD solution with conjugation efficiency of 61 %.

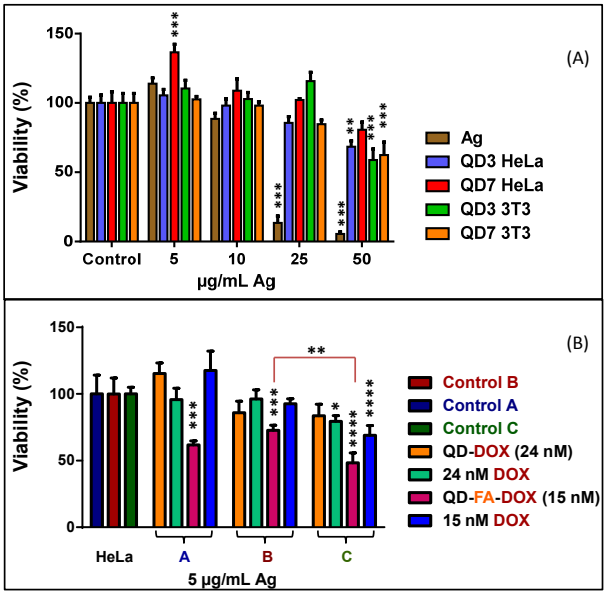

Fig. 4 (A) *In vitro* viability of NIH/3T3 and HeLa cells incubated 24h with QD3, QD7 and $AgNO_3$ at different doses based on Ag^+ ion concentration (5, 10, 25 and 50 µg Ag/mL). Five controls represent the untreated control cells in each plate. **(B)** *In vitro* viability of HeLa cells incubated 24h with QD-FA-DOX at 5 µg Ag/mL (0.418 mg QD/mL), QD-DOX at 5 µg Ag/mL (0.336 mg QD/mL) and free DOX (15 and 24 nM). Incubation of nanoparticles and DOX was performed (A) in complete DMEM, (B) in folic acid free medium with 2 mM folic acid and (C) in folic acid free medium. Three controls represent the untreated control cells in each plate. Statistical analysis was done with one-way ANOVA with Tukey's multiple comparison at $p < 0.05$(*), $p < 0.01$ (**), $p < 0.001$ (***) and $p < 0.0001$ (****)

Doxorubicin (DOX) is one of the most widely used cancer chemotherapeutic drugs with antigenic activity.[50, 51] DOX was electrostatically bound to both QD and QD-FA with 1.7 and 4.2 % loading efficiency. DOX amount loaded to QDs were calculated from the emission peak of DOX at 595 nm using a calibration curve created for DOX (Figure S6 in the SI). Ag_2S-PEG (QD-DOX) and Ag_2S-PEG-FA (QD-FA-DOX) nanoparticles have 320 nM and 160 nM DOX, respectively. DOX loading did not change the stability or the hydrodynamic size of the particles significantly, most probably due to not so high loading (Table S2 in the SI).

Journal of Materials Chemistry B Accepted Manuscript

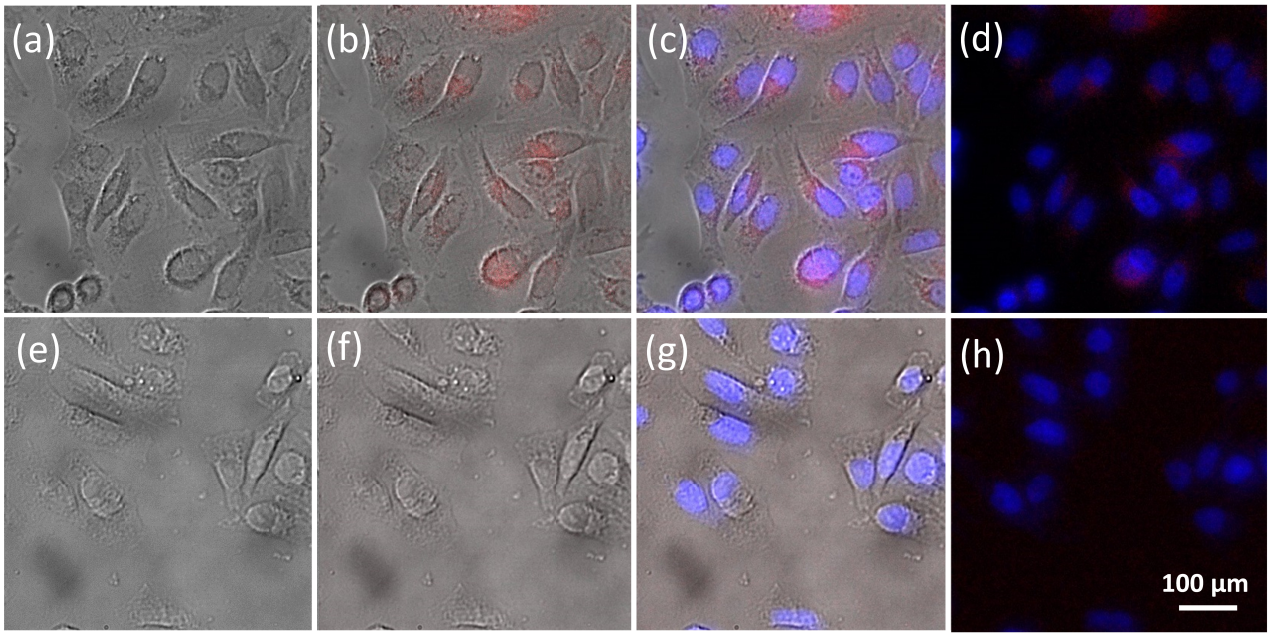

Fig. 5. Inverted fluorescence microscopy images of HeLa cells incubated with QD6 (28 µg Ag /mL, 3.6 mg QD/mL, 6 h incubation) (a-d) and control cells (e-h). Images (a) and (e) are bright field, (b) and (f) are merged bright field and NIR images, (c) and (d) are merged images from DAPI, NIR and bright field, (d) and (h) are merged images from DAPI and NIR filters.

In vitro cell viability studies were repeated with QD-FA-DOX and QD-DOX, to evaluate the potential of these QDs as targeted drug delivery vehicles, using the HeLa cells with overexpressed FA receptor. This study was performed with a low dose of QD at 5 µg/mL Ag concentration. In parallel, toxicity of free DOX at concentrations identical to those brought by the QDs were used (15 and 24 nM DOX). In case A (Figure 4B), where complete DMEM medium was used, statistically the only toxic material is the QD-FA-DOX with viability around 60 %. Amount of DOX that is conjugated to the nanoparticle at this dose did not cause any significant toxicity if provided as a free drug. This is very important since it indicates that loading of DOX to non-toxic nanoparticles and selective delivery to the cancer cells via folate targeting, increases the efficacy of the drug. Alternatively, in case B, folic acid free medium was used for the cell culture, followed by addition of free folic acid solution (2 mM) into the medium to saturate folate receptors of the cells before QDs or free DOX were added to cells.[52] Again, QD-FA-DOX showed the only statistically significant drop in the viability of cells, confirming the previous conclusions. In case C, folic acid free medium was used and the receptors were not saturated with free FA. This time, both free DOX at both concentrations (15 and 24 nM) and QD-FA-DOX showed significant toxicity. Folate targeted QD-FA-DOX showed about 50 % drop in the viability with only 15 nM DOX. This means that QD-FA-DOX carries the toxic drug into the cells more effectively than QD-DOX. In addition, the difference between the viability of cells incubated with QD-FA-DOX in case B (folate receptors saturated before QD addition) and case C (free folate receptors) is significant, confirming the action of FA in targeted delivery of QDs. Overall, these results suggest that higher toxicity to cancer cell lines with lower DOX loading can be achieved via targeted delivery of these QDs using FA conjugation. Same study was performed with QDs at 10 µg/mL Ag dosage and same outcomes were obtained (Figure S7 in the SI).

***In vitro* Optical Imaging of the Ag_2S-PEG NIRQDs.**

In order to visually confirm the internalization of QDs by the cells and evaluate their use as optical probes, cells incubated with the nanoparticles were imaged under Inverted Fluorescence Microscope. Typically, the sensitivity of the detectors used in such microscopes fall around 30% after 900 nm. Yet, internalization of QD6 (emission maximum at 930 nm) by the cells was successfully detected using a NIR filter due to very high quantum yield of the particles. In images shown in Figure 5, the red colour represents the emission originating from QD6 (using the NIR filter) and blue colour represents the cell nucleus stained with DAPI (using DAPI filter). Comparison of images in Figure 5a-d with images obtained from control cells (Figure 5e-h) shows the effective internalization of QDs by the HeLa cells, localization in cytoplasm and no nuclear uptake. More importantly, these images confirm the potential of these QDs as strong optical cellular probes. Considering the working range of the detector, most probably detection is obtained from the low wavelength end of the emission tail and where the sensitivity of the detector is low. With a more appropriate detection system, even a stronger luminescence signal can be detected. A similar study was performed with DOX loaded particles, as well (Figure 6). Emission maximum of DOX is around 600 nm. Therefore, CY3 filter was used to detect the

Journal of Materials Chemistry B Accepted Manuscript

This journal is © The Royal Society of Chemistry 20xx

Please do not adjust margins

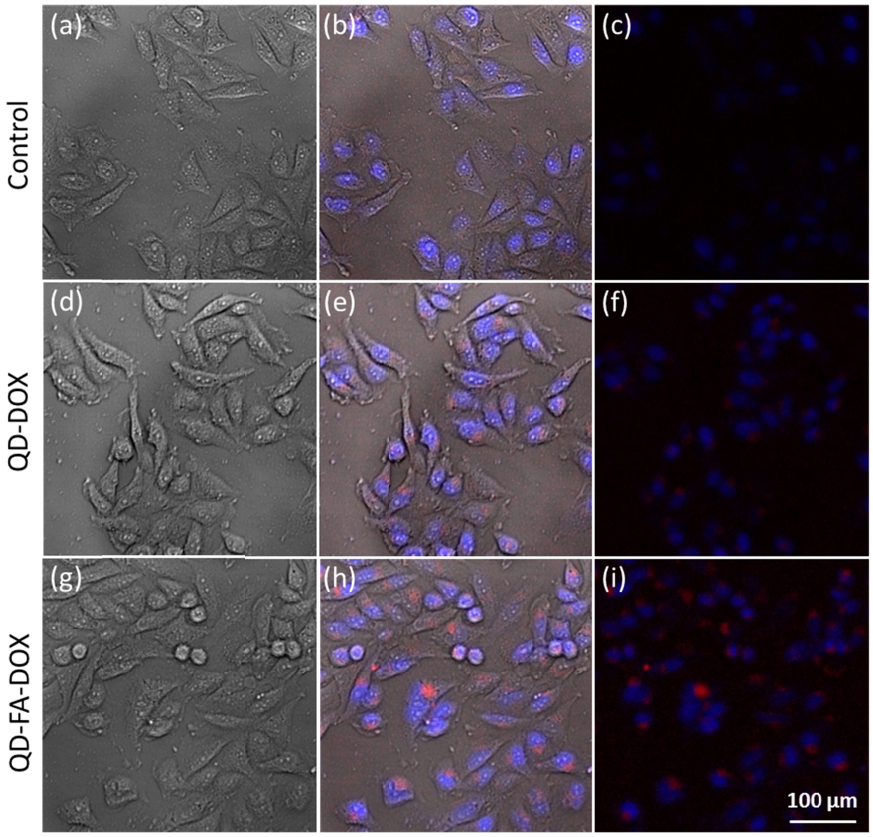

Fig. 6 Inverted fluorescence microscopy images of control HeLa cells (a-c) and HeLa cells after 6h incubation with QD-DOX (10 µg Ag /mL, 0.672 mg QD/mL) (d-f) and QD-FA-DOX (10 µg Ag /mL, 0.836 mg QD/mL) (g-i). Images a,d and g are bright field; b,e and h are merged images from DAPI, CY3 filters and bright field; c,f and i are merged images from DAPI and CY3 filters.

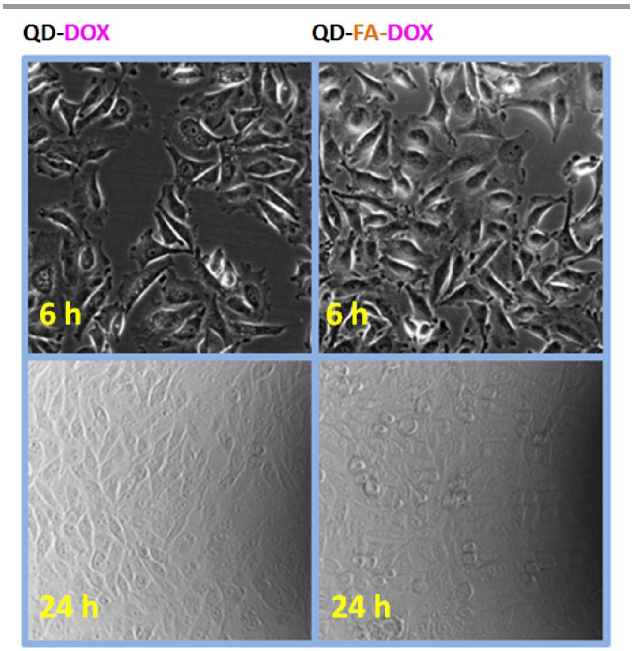

Fig.7 Inverted fluorescence microscopy images showing the morphology of HeLa cells incubated with QD-DOX (10 µg Ag/mL, 0.672 mg QD/mL), and QD-FA-DOX (10 µg Ag/mL, 0.836 mg QD/mL) after 6 and 24 hours incubation.

emission originating from DOX, which is the red colour in the images (Figure 6). After 6 h incubation with QD-DOX and QD-FA-DOX at 10 µg/mL Ag dose, cells were still healthy and it seems like QD-FA-DOX (Figure 6 h and i) was internalized more than QD-DOX (Figure 6e and f), which is in agreement with the toxicity data. After 24 hours incubation, HeLa cells incubated with QD-DOX were still healthy, but those incubated with QD-FA-DOX were mostly dead (Figure 7). These images also refer to improved uptake of particles, and hence the drug, with the folic acid tagged QDs, as desired.

Conclusions

Here, we have demonstrated a simple, one pot synthesis of highly luminescent PEG coated Ag_2S QDs that are luminescent in the medical window between 847-930 nm with QY as high as 65 %, using thiolated PEG coating of 2000 and 5000 g/mol. Method is simple enough to produce functional PEG coatings such as carboxylic acid terminated QDs for conjugation of specific tags such as folic acid, peptides, proteins, etc. QD size, emission wavelength and QY can be tailored with the ratio of the precursors, PEG molecular weight and reaction pH. PEG5000 and reaction pH of 3 show a dramatic enhancement in the luminescence intensity. To the best of our knowledge this is the first time such an effect has been reported. Ag_2S-

Journal of Materials Chemistry B Accepted Manuscript

Please do not adjust margins

PEG QDs are well tolerated by both a cancer cell line (HeLa) and mouse fibroblast (NIH/3T3) at exceptionally high doses (mg range) of particles. Internalized particles, generates a strong NIR signal which can be even improved further with a more suitable detector where emission at the peak maximum rather than the tail can be imaged.

High molecular weight of PEG allow DOX loading to QDs. Ag_2S-PEG QDs tagged with FA and loaded with DOX showed excellent drug efficiency coupled with receptor mediated uptake which allows selective delivery of particles to target site, while PEG only coating, increases blood-circulation and decreases fast uptake of particles. About 50 % drop in cell viability in 24h achieved with as low as 15 nM DOX carried with 0.418 mg/mL QDs is remarkable. Minimizing the effective dose of the chemotherapeutic agent is very important. Usually, loading the toxic drug into a relatively safer drug-carriers aims to achieve low effective dose and site specific delivery, when possible.[53] These results are very promising from this perspective. A recent study reported about 40 % drop in the viability of MDA-MB-231 cells with Ag_2S QDs coated with dodecanethiol/C18PMHPEG bilayer with 20 μM DOX (corresponding to 10 μg/mL Ag_2S concentration) in 72h. They have achieved similar toxicity with Ag_2S to free DOX between 10-150 μM DOX concentrations.[36] Here, we have achieved much higher toxicity with much lower DOX dose.

We strongly believe that these particles are promising theranostic QDs, prepared in a very simple method.

Acknowledgements

The authors thank Koc University for funding, to Cansu Yıldırım at KUYTAM-Koç University for XRD, to Dr. Ibrahim Hocaoglu at Koc University for ICP measurements, to Assoc. Prof. Ozgur Birer for handmade PL instrument and Dr. Rouhollah Khodadust for his help with Image J software.

References

1. B. Chertok, A. E. David and V. C. Yang, *Biomaterials*, 2010, **31**, 6317-6324.
2. C. L. Huang, C. C. Huang, F. D. Mai, C. L. Yen, S. H. Tzing, H. T. Hsieh, Y. C. Lingd and J. Y. Chang, *Journal of Materials Chemistry B*, 2015, **3**, 651-664.
3. V. Bagalkot, L. Zhang, E. Levy-Nissenbaum, S. Jon, P. W. Kantoff, R. Langer and O. C. Farokhzad, *Nano Lett*, 2007, **7**, 3065-3070.
4. H. S. Han, E. Niemeyer, Y. H. Huang, W. S. Kamoun, J. D. Martin, J. Bhaumik, Y. C. Chen, S. Roberge, J. Cui, M. R. Martin, D. Fukumura, R. K. Jain, M. G. Bawendi and D. G. Duda, *Proceedings of the National Academy of Sciences of the United States of America*, 2015, **112**, 1350-1355.
5. S. C. Baetke, T. Lammers and F. Kiessling, *Brit J Radiol*, 2015, **88**.
6. Y. Wang, E. Cai, T. Rosenkranz, P. H. Ge, K. W. Teng, S. J. Lim, A. M. Smith, H. J. Chung, F. Sachs, W. N. Green, P. Gottlieb and P. R. Selvin, *Bioconjugate Chemistry*, 2014, **25**, 2205-2211.
7. J. K. Jaiswal and S. M. Simon, *Trends in Cell Biology*, 2004, **14**, 497-504.
8. H. N. Yang, J. S. Park, S. Y. Jeon, W. Park, K. Na and K. H. Park, *Biomaterials*, 2014, **35**, 8439-8449.
9. C. E. Probst, P. Zrazhevskiy, V. Bagalkot and X. H. Gao, *Adv Drug Deliver Rev*, 2013, **65**, 703-718.
10. X. H. Gao, L. L. Yang, J. A. Petros, F. F. Marshal, J. W. Simons and S. M. Nie, *Current Opinion in Biotechnology*, 2005, **16**, 63-72.
11. M. Geszke, M. Murias, L. Balan, G. Medjandi, J. Korczynski, M. Moritz, J. Lulek and R. Schneider, *Acta Biomaterialia*, 2011, **7**, 1327-1338.
12. A. C. Poulose, S. Veeranarayanan, M. S. Mohamed, S. Raveendran, Y. Nagaoka, Y. Yoshida, T. Maekawa and D. S. Kumar, *Journal of Fluorescence*, 2012, **22**, 931-944.
13. I. Hocaoglu, F. Demir, O. Birer, A. Kiraz, C. Sevrin, C. Grandfils and H. Y. Acar, *Nanoscale*, 2014, **6**, 11921-11931.
14. W. W. Yu, L. H. Qu, W. Z. Guo and X. G. Peng, *Chem Mater*, 2003, **15**, 2854-2860.
15. R. G. Aswathy, Y. Yoshida, T. Maekawa and D. S. Kumar, *Analytical and Bioanalytical Chemistry*, 2010, **397**, 1417-1435.
16. P. Sharma, S. Brown, G. Walter, S. Santra and B. Moudgil, *Adv Colloid Interfac*, 2006, **123**, 471-485.
17. S. Stolik, J. A. Delgado, A. Perez and L. Anasagasti, *Journal of Photochemistry and Photobiology B-Biology*, 2000, **57**, 90-93.
18. H. Y. Chen, S. S. Cui, Z. Z. Tu, J. Z. Ji, J. Zhang and Y. Q. Gu, *Photochem Photobiol*, 2011, **87**, 72-81.
19. T. Jin, F. Fujii, Y. Komai, J. Seki, A. Seiyama and Y. Yoshioka, *Int J Mol Sci*, 2008, **9**, 2044-2061.
20. M. Q. Sun, Q. L. Yu, M. Y. Hu, Z. W. Hao, C. D. Zhang and M. C. Li, *J Hazard Mater*, 2014, **273**, 7-16.
21. A. M. Derfus, W. C. W. Chan and S. N. Bhatia, *Nano Lett*, 2004, **4**, 11-18.
22. N. Lewinski, V. Colvin and R. Drezek, *Small*, 2008, **4**, 26-49.
23. J. Lee, K. Ji, J. Kim, C. Park, K. H. Lim, T. H. Yoon and K. Choi, *Environmental Toxicology*, 2010, **25**, 593-600.
24. J. M. Tsay and X. Michalet, *Chemistry & Biology*, 2005, **12**, 1159-1161.
25. W. W. Yu, E. Chang, R. Drezek and V. L. Colvin, *Biochemical and Biophysical Research Communications*, 2006, **348**, 781-786.
26. P. F. Zhang and H. X. Han, *Colloid Surface A*, 2012, **402**, 72-79.
27. T. J. Daou, L. Li, P. Reiss, V. Josserand and I. Texier, *Langmuir*, 2009, **25**, 3040-3044.
28. M. Lu, W. D. Zhang, Y. K. Gai, T. Yang, P. Ye, G. Yang, X. Ma and G. Y. Xiang, *New J Chem*, 2014, **38**, 4519-4526.
29. R. G. Xie, K. Chen, X. Y. Chen and X. G. Peng, *Nano Res*, 2008, **1**, 457-464.
30. D. W. Deng, Y. Q. Chen, J. Cao, J. M. Tian, Z. Y. Qian, S. Achilefu and Y. Q. Gu, *Chem Mater*, 2012, **24**, 3029-3037.
31. M. Helle, E. Cassette, L. Bezdetnaya, T. Pons, A. Leroux, F. Plenat, F. Guillemin, B. Dubertret and F. Marchal, *Plos One*, 2012, **7**.
32. I. Hocaoglu, M. N. Cizmeciyan, R. Erdem, C. Ozen, A. Kurt, A. Sennaroglu and H. Y. Acar, *Journal of Materials Chemistry*, 2012, **22**, 14674-14681.
33. Y. Zhang, G. S. Hong, Y. J. Zhang, G. C. Chen, F. Li, H. J. Dai and Q. B. Wang, *Acs Nano*, 2012, **6**, 3695-3702.

Journal of Materials Chemistry B Accepted Manuscript

This journal is © The Royal Society of Chemistry 20xx

Please do not adjust margins

34. R. J. Gui, J. Sun, D. X. Liu, Y. F. Wang and H. Jin, *Dalton T*, 2014, **43**, 16690-16697.
35. M. L. Schipper, G. Iyer, A. L. Koh, Z. Cheng, Y. Ebenstein, A. Aharoni, S. Keren, L. A. Bentolila, J. Q. Li, J. H. Rao, X. Y. Chen, U. Banin, A. M. Wu, R. Sinclair, S. Weiss and S. S. Gambhir, *Small*, 2009, **5**, 126-134.
36. F. Hu, C. Y. Li, Y. J. Zhang, M. Wang, D. M. Wu and Q. B. Wang, *Nano Res*, 2015, **8**, 1637-1647.
37. Y. Zhang, Y. J. Zhang, G. S. Hong, W. He, K. Zhou, K. Yang, F. Li, G. C. Chen, Z. Liu, H. J. Dai and Q. B. Wang, *Biomaterials*, 2013, **34**, 3639-3646.
38. Y. P. Du, B. Xu, T. Fu, M. Cai, F. Li, Y. Zhang and Q. B. Wang, *Journal of the American Chemical Society*, 2010, **132**, 1470-+.
39. A. Dubavik, V. Lesnyak, W. Thiessen, N. Gaponik, T. Wolff and A. Eychmuller, *J Phys Chem C*, 2009, **113**, 4748-4750.
40. A. Dubavik, E. Sezgin, V. Lesnyak, N. Gaponik, P. Schwille and A. Eychmuller, *Acs Nano*, 2012, **6**, 2150-2156.
41. L. Brus, *Journal of Physical Chemistry*, 1986, **90**, 2555-2560.
42. L. E. Brus, *Journal of Chemical Physics*, 1984, **80**, 4403-4409.
43. H. Li, W. Y. Shih and W. H. Shih, *Industrial & Engineering Chemistry Research*, 2007, **46**, 2013-2019.
44. F. D. Duman, I. Hocaoglu, D. G. Ozturk, D. Gozuacik, A. Kiraz and H. Y. Acar, *Nanoscale*, 2015, **7**, 11352-11362.
45. R. J. Gui, A. J. Wan, X. F. Liu, W. Yuan and H. Jin, *Nanoscale*, 2014, **6**, 5467-5473.
46. K. P. Bhandari, H. Choi, S. Jeong, H. Mahabaduge and R. J. Ellingson, *Appl Phys Lett*, 2014, **105**.
47. T. Niidome, M. Yamagata, Y. Okamoto, Y. Akiyama, H. Takahashi, T. Kawano, Y. Katayama and Y. Niidome, *Journal of Controlled Release*, 2006, **114**, 343-347.
48. D. Feng, Y. C. Song, W. Shi, X. H. Li and H. M. Ma, *Analytical Chemistry*, 2013, **85**, 6530-6535.
49. J. Sudimack and R. J. Lee, *Adv Drug Deliver Rev*, 2000, **41**, 147-162.
50. W. Arap, R. Pasqualini and E. Ruoslahti, *Science*, 1998, **279**, 377-380.
51. V. Yagublu, N. Caliskan, A. L. Lewis, R. Jesenofsky, L. Gasimova, J. M. Lohr and M. Keese, *Pancreatology*, 2013, **13**, 79-87.
52. H. Chen, R. Ahn, J. Van den Bossche, D. H. Thompson and T. V. O'Halloran, *Molecular Cancer Therapeutics*, 2009, **8**, 1955-1963.
53. F. M. Kievit, F. Y. Wang, C. Fang, H. Mok, K. Wang, J. R. Silber, R. G. Ellenbogen and M. Q. Zhang, *Journal of Controlled Release*, 2011, **152**, 76-83.

Journal of Materials Chemistry B Accepted Manuscript